

Observation of soft magnetorotons in bilayer quantum Hall ferromagnets

Stefano Luin,^{1,2} Vittorio Pellegrini,¹ Aron Pinczuk,^{2,3} Brian S. Dennis,² Loren N. Pfeiffer,² and Ken W. West²

¹*NEST-INFM and Scuola Normale Superiore, Piazza dei Cavalieri 7, I-56126 Pisa (Italy)*

²*Bell Labs, Lucent Technologies, Murray Hill, New Jersey 07974*

³*Dept. of Physics, Dept. of Appl. Phys. and Appl. Math,
Columbia University, New York, New York 10027*

(Dated: November 13, 2018)

Inelastic light scattering measurements of low-lying collective excitations of electron double layers in the quantum Hall state at total filling $\nu_T=1$ reveal a deep magnetoroton in the dispersion of charge-density excitations across the tunneling gap. The roton softens and sharpens markedly when the phase boundary for transitions to highly correlated compressible states is approached. The findings are interpreted with Hartree-Fock evaluations that link soft magnetorotons to enhanced excitonic Coulomb interactions and to quantum phase transitions in the ferromagnetic bilayers.

PACS numbers: 73.43.Lp, 78.30.-j, 73.21.-b

The quantum Hall states of the two-dimensional electron gas (2DEG) occur in high perpendicular magnetic fields that quantize the kinetic energy into discrete, highly-degenerate Landau levels (LLs). The energy scale for Coulomb interactions is here $e^2/\epsilon l_B$, where $l_B = \sqrt{\hbar c/eB}$ is the magnetic length and B the perpendicular magnetic field. The neutral quasiparticle-quasihole excitations carry the fingerprints of electron interactions [1, 2]. Low-lying collective modes of energies $\omega(\mathbf{q})$ and in-plane wave vector \mathbf{q} are linked to the condensation into highly correlated states that emerge in the presence of strong electron interactions. Theoretical dispersions $\omega(\mathbf{q})$ display characteristic magnetoroton (MR) minima at finite wave-vectors ($q \sim l_B^{-1}$) that are due to excitonic binding terms of the Coulomb interactions in the neutral pairs [3, 4]. It has been predicted that MRs can soften and create instabilities leading to quantum phase transitions that transform the ground-states into highly correlated electron phases [3, 5, 6, 7, 8, 9].

Coupled electron bilayers at total Landau level filling factor $\nu_T=1$ exhibit a rich quantum phase diagram due to the interplay of transition energies Δ_{SAS} across the tunneling gap with intra- and inter-layer interactions [5, 8, 10, 11, 12, 13]. Interactions drive quantum phase transitions from the incompressible ferromagnetic quantized Hall phase, stable at low inter-layer spacing d or large Δ_{SAS} , to a compressible phase that results from the collapse of the many-body tunneling gap. In current theories the phase transitions are linked to soft roton instabilities in the charge-density-excitations (CDE) across the tunneling gap [5, 8]. Within the Hartree-Fock framework the magnetoroton instability is related to intra-layer interactions that lead to large excitonic bindings between quasiparticles and quasiholes.

Recent experimental studies of coupled electron double layers in $\nu_T=1$ ferromagnetic states focus on the very low Δ_{SAS} region of the phase diagram, where inter-layer Coulomb correlations are important. These studies have displayed enhanced zero-bias inter-layer tunnel-

ing characteristics and anomalous quantized Hall drag [14, 15, 16]. These remarkable results are interpreted as evidence of a Goldstone mode in the incompressible phase and of condensation of the bilayers into many-body exciton phases. Experiments that probe dispersive collective excitations and their softening as a function of Δ_{SAS} and d could provide direct evidence of the impact of excitonic terms of interactions in the quantum phase transitions of the ferromagnetic bilayers.

Resonant inelastic light scattering methods have been employed in studies of very low-energy $q \sim 0$ tunneling excitations with spin reversal in electron bilayers at even integer values of ν_T [17]. These studies have revealed that excitonic interactions can drive changes in the quantum ground state and finite temperature transitions [18, 19]. We report here light scattering experiments that offer direct evidence of soft magnetorotons in the CDE modes across the tunneling gap of coupled electron bi-layers at $\nu_T=1$. MR modes at wavevectors $q \sim l_B^{-1}$ and modes with larger wave vectors can be accessed in the resonant light scattering experiments due to breakdown of wave vector conservation. The light scattering spectra with breakdown of wave vector conservation show maxima at the critical points in the mode dispersion [20].

We find that the light scattering spectra of low-lying modes typically display three bands of CDE. One is the $q \sim 0$ excitation. The other two are assigned to the CDE modes at critical points in the dispersion. The lowest of these two is the critical point at the magnetoroton minimum with $q \sim l_B^{-1}$, and the higher energy band is the large density of states of modes with $q \gg l_B^{-1}$. The MR mode softens markedly when Δ_{SAS} is reduced and the double-layer system approaches the incompressible-compressible phase boundary. Close to this boundary the MR occurs at an energy significantly lower than Δ_{SAS} . Magnetoroton spectral lineshapes and temperature dependences display striking differences with those of the long-wavelength modes. Close to the phase boundary the MR band shows extreme narrowing to a width of less

than $70 \mu\text{eV}$ at temperatures $T \simeq 60\text{mK}$.

We have interpreted these results within the framework of a time-dependent Hartree-Fock approximation (TD-HFA) that includes breakdown of wave vector conservation in light scattering. The calculations reproduce the MR energies and indicate that the sharpening of the MR band reflects significant changes in the mode dispersion and matrix element near the incompressible-compressible phase boundary. These results uncover significant evidence that softening of the rotons play major roles in the phase transitions of bilayers at $\nu_T=1$ and suggest a leading role for excitonic Coulomb interactions in transitions between highly correlated phases.

Results obtained in two modulation doped double quantum wells (DQWs) grown by molecular beam epitaxy are presented. Samples consist of two 18 nm GaAs wells separated by an undoped $\text{Al}_{0.1}\text{Ga}_{0.9}\text{As}$ barrier (7.5 nm for sample A and 6.23 nm for sample B). Figure 1(a) shows the schematic profile of the bottom of the conduction band in the DQWs. Dotted lines represent the energy of lowest symmetric and antisymmetric states. By design the samples have the relatively high Δ_{SAS} of 0.32 meV in sample A and 0.58 meV in sample B. Magneto-transport confirms that both samples are in the quantum Hall side of the phase diagram as shown in Fig. 1(b). Total sheet densities are $1.2 \times 10^{11} \text{ cm}^{-2}$ in sample A and $1.1 \times 10^{11} \text{ cm}^{-2}$ in sample B with mobilities larger than $10^6 \text{ cm}^2/\text{Vs}$. Inelastic light scattering spectra are obtained in a back-scattering geometry with light propagating along the magnetic field. Samples are mounted in a $^3\text{He}/^4\text{He}$ dilution cryo-magnetic system with optical windows, at a small tilt angle (20 degrees) with respect to the incoming laser light. Accessible temperatures are in the range 50 mK–1.4 K. For these measurements the optical emission of a dye laser is tuned to a frequency ω_I close to the fundamental interband transitions of the DQW. Incident power densities are kept below $\lesssim 10^{-4} \text{ W/cm}^2$, and spectra are recorded using a double monochromator, CCD multichannel detection and spectral resolution of $15 \mu\text{eV}$.

The C0 bands shown in Fig. 1(c) have similar energies and widths in the two samples, and also occur in spectra obtained at $B=0$. On this basis they are assigned to $q \rightarrow 0$ CDE modes [21]. The structures labelled MR are remarkably different in the two samples. They appear as a weak shoulder with a cutoff at 0.65 meV in sample B, and as a sharp low-energy peak at 0.22 meV in sample A. The spin wave (SW) at the Zeeman energy $E_Z = 0.11 \text{ meV}$ also occurs in the low-energy spectra of sample A. Figure 2(a) shows a resonant enhancement profile measured in sample B that reveals a characteristic outgoing resonance with the higher optical interband transition of the luminescence peak labelled L. The spectra from sample A display similar outgoing resonances.

Figures 2(b) and (c) show the calculated dispersion $\omega_C(q)$ obtained within TDHFA and the $|M(q)|^2$ factor

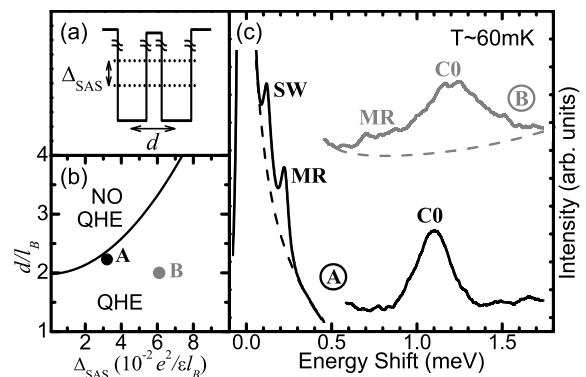


FIG. 1: (a) Schematic representation of the double quantum well and of the two lowest confined states. (b) Phase diagram for the incompressible (QHE)-compressible (NO QHE) states of the bilayer at $\nu = 1$ (from Refs. 12, 13); the dots mark the positions of samples A and B. (c) Inelastic light scattering spectra from sample A (black curves and labels) and B (gray curve and labels). SW is the spin-wave, C0 is the $q \sim 0$ CDE mode, and MR the magnetoroton minimum.

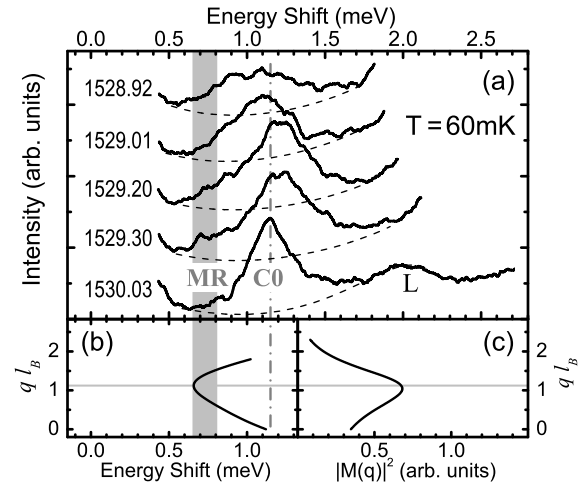


FIG. 2: (a) Inelastic light scattering spectra at $\nu_T=1$ obtained in sample B for different incident photon energies (in meV). The band labelled L is luminescence. (b) Calculated dispersion of CDE modes across the tunneling gap. (c) Calculated matrix element $M(q)$ for inelastic light scattering. The vertical dash-dotted line shows the energy of the $q=0$ CDE mode; the gray area indicates contributions of large wavevector modes with energies down to the roton minimum. The horizontal thin lines in (b) and (c) are at the magnetoroton (MR) wave vector.

that enters in the expression of the dynamic structure factor $S(q, \omega)$

$$S(q, \omega) \propto \frac{|M(q)|^2 \omega_C(q) \omega \Gamma}{[\omega^2 - \omega_C^2(q)]^2 + \omega^2 \Gamma^2}, \quad (1)$$

where Γ is the homogeneous broadening [10, 20]. This TDHFA model defines a phase boundary for the instability at values of d/l_B lower than the experimental ones

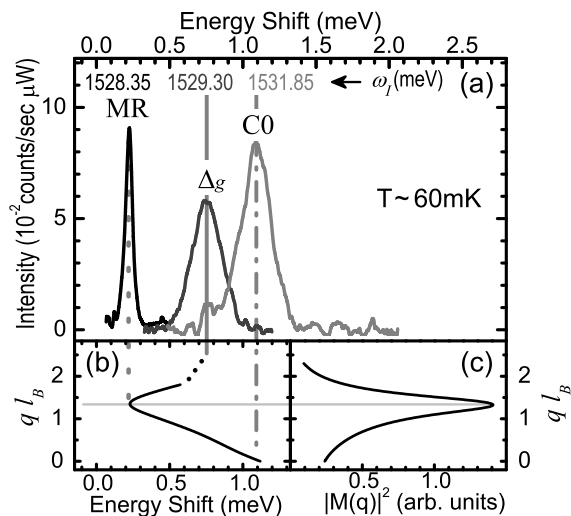


FIG. 3: (a) Light scattering bands of CDE in sample A at $\nu_T=1$. The estimated background due to luminescence and laser has been subtracted. The incident photon energies ω_I are indicated in meV. Δ_g labels the $q \rightarrow \infty$ mode. (b) Calculated dispersion of CDE modes; extrapolation to the long wave-vector limit is shown as dotted line. (c) Calculated inelastic light scattering “matrix element”. Vertical lines in (a) show the peak position of CDE modes. The horizontal line in (b) and (c) is at the MR wave vector.

by a factor of two. To correct for this discrepancy the d/l_B parameters used in the calculations have been consistently adjusted to match the parameters in our two samples. The matrix element $|M(q)|^2$ acts as an oscillator strength for inelastic light scattering by the collective excitations. At the lowest order, the light-scattering cross section is proportional to the product of $S(q, \omega)$ and a factor that incorporates resonant enhancements and optical matrix elements. $S(q, \omega)$ is used to evaluate the intensities of inelastic light scattering by CDE modes of different wave vectors. In this evaluation the extent of breakdown of wavevector conservation is treated as in Ref. [20].

The comparison of spectra of sample B in Fig. 2 with the TDHFA calculation confirms the assignment of the band labelled C0 at 1.13 meV as the long wavelength CDE shifted above Δ_{SAS} by dynamical many-body contributions. This peak is observed at temperatures of up to 1.4 K and over a relatively broad range of ω_I and explored magnetic fields ($0.7 < \nu_T < 1.2$). The low-energy shoulder with a cutoff at MR is observed only in a very narrow range of ω_I and for B values very close to $\nu_T=1$. This structure is assigned to resonant inelastic light scattering processes with breakdown of wave vector conservation. The lowest measured energy in this relatively broad structure represents the magnetoroton in the dispersion of CDE modes.

The marked softening of the MR mode in sample A seen in Fig. 1(c) suggests links between soft magnetoro-

tons and the incompressible-compressible quantum phase transition at $\nu_T = 1$. Figure 3(a) shows resonant inelastic light spectra of CDE modes in sample A with conventional subtraction of the background due to the laser and to the main magneto-luminescence. The results display clearly the three bands of CDE collective modes. In addition to the CDE at $q \approx 0$ (C0, dash-dotted line at 1.08 meV) two lower-energy excitations are clearly seen. The lowest energy mode at 0.22 meV is assigned to the MR critical point in the dispersion. Its energy is much lower than the MR in sample B. The MR in Fig. 3(a) is extremely narrow, with a full width at half maximum (FWHM) of ~ 0.06 meV, which is a factor of three smaller than the FWHM of the C0 band. The peak at 0.75 meV, labelled Δ_g , is the large wavevector CDE excitation. The Δ_g and MR modes display a marked sensitivity to deviations of magnetic field values from $\nu_T=1$ in a manner that is similar to the QH states. The assignments of the C0 and MR bands in Fig. 3(a) are also supported by the calculated dispersions shown in Fig. 3(b).

Significant insights are gained from a study of the q -dependence of $|M(q)|^2$. Comparison of the calculation for sample A in Fig. 3(c) with that for sample B in Fig. 2(c) indicates that on reduction of Δ_{SAS} , approaching the phase transition, $|M(q)|^2$ tends to peak sharply at the MR wavevector. These results suggest that, by predicting the softening and sharpening of the magnetoroton, the TDHFA, a leading-order many body calculation, provides a framework to analyze manifestations of interactions that eventually lead to the soft-mode driven quantum phase transition [22].

The interactions that interpret the softening and narrowing of the MR mode in sample A would eventually drive the incompressible-compressible transition upon further reduction of Δ_{SAS} . These interactions are related to the excitonic Coulomb term that creates the roton in the CDE mode dispersion. It is conceivable that such excitonic binding increases at lower values of Δ_{SAS} due to enhanced overlap between the single-particle wavefunctions of symmetric and antisymmetric states.

The TDHFA interprets the energies, linewidths and intensities of MRs in the light-scattering spectra. The results support the picture that the ground state of the bilayers at $\nu_T=1$ evolves towards a broken-symmetry state caused by the collapse of the energy of tunneling excitations [5, 8, 10]. The marked narrowing of the MR band and its interpretation within the TDHFA suggest that the transition might be characterized by a roton wave vector $q_R \sim l_B^{-1}$. Our results also support a scenario in which the instability is associated with the condensation of neutral excitons [14, 15, 16, 23]. The exciton fluid would be linked to large densities of extremely low energy magnetoroton modes of the incompressible phase.

The MR temperature dependence measured in sample A suggests that a highly correlated QH state may occur near the phase boundary. Figure 4 shows two rep-

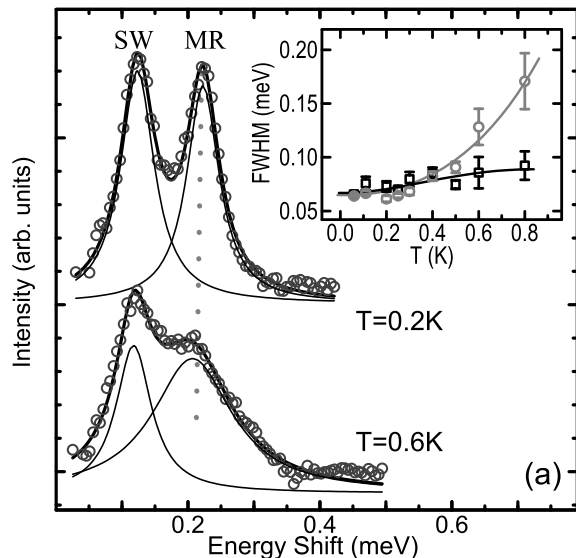


FIG. 4: Open circles show the temperature dependence of light scattering spectra in sample A. The background subtraction is as in Fig. 3(a). The solid lines are results of fits with two Lorentzians. Inset: temperature dependence of the FWHM for the spin-wave (SW) peak at the Zeeman energy (black empty squares) and the MR peak (gray empty circles). The solid lines are guides for the eyes and the error bars are standard deviations for results on different measurements and with different background subtractions.

representative spectra in which both SW and MR modes are observed. The linewidth of the two excitations have the very different temperature dependence shown in the inset to Fig. 4. The FWHM's are obtained from Lorentzian fits (solid lines in Fig. 4). For temperatures above 0.8K the MR mode can no longer be observed and minor changes occur in the SW peak. Similar temperature dependences characterize the $q \rightarrow \infty$ (Δ_g) mode and the magneto-transport data. The characteristic temperature is here much smaller than Δ_g and more than a factor of three below the MR energy in sample A. The $q \sim 0$ (C0) mode is temperature-independent up to 1.4K. A similar anomalous behavior observed in activated magneto-transport was interpreted as evidence for a finite-temperature transition towards an uncorrelated state [24, 25]. The evolution of MR linewidth shown in the inset of Fig. 4 supports this conclusion. From the smooth increase of the linewidth as a function of temperature, it can be argued that thermal fluctuations destroy the incompressible state and trigger a continuous transition at finite temperature. Thermal excitation of long wavelength SW modes, fixed by Larmor theorem at the Zeeman energy,

could play roles in such transition.

In conclusion, we observed magnetorotons in the dispersions of low-lying charge-density excitations in ferromagnetic electron bilayers at $\nu_T=1$. Soft and sharp magnetorotons exist in close proximity to the incompressible-to-compressible quantum phase transition. The key features of the experiments have been interpreted within time-dependent Hartree-Fock approximation. These results suggest direct links between transitions in the electron quantum ground-state and the low-lying dispersive collective modes.

We are grateful to S. Das Sarma, E. Demler, S. M. Girvin, S.H. Simon and D.W. Wang for critical reading of the manuscript and significant suggestions. Partial support from CNR (Consiglio Nazionale delle Ricerche), INFN/E (Istituto Nazionale per la Fisica della Materia, section E) and MIUR is also acknowledged.

-
- [1] S. Das Sarma and A. Pinczuk, eds., *Perspectives in Quantum Hall Effect* (Wiley, New York, 1997).
 - [2] R. E. Prange and S. M. Girvin, eds., *The Quantum Hall Effect* (Springer-Verlag, New York, 1987).
 - [3] S. M. Girvin et al., Phys. Rev. B **33**, 2481 (1986).
 - [4] C. Kallin and B. I. Halperin, Phys. Rev. B **30**, 5655 (1984).
 - [5] A. H. MacDonald et al., Phys. Rev. Lett. **65**, 775 (1990).
 - [6] Y. N. Joglekar and A. H. MacDonald, Phys. Rev. B **65**, 235319 (2002).
 - [7] H. A. Fertig, Phys. Rev. B **40**, 1087 (1989).
 - [8] L. Brey, Phys. Rev. Lett. **65**, 903 (1990).
 - [9] R. K. Kamilla and J. K. Jain, Phys. Rev. B **55**, R13417 (1997).
 - [10] L. Brey, Phys. Rev. B **47**, 4585 (1993).
 - [11] G. S. Boebinger et al., Phys. Rev. Lett. **64**, 1793 (1990).
 - [12] Kun Yang et al., Phys. Rev. B **54**, 11644 (1996).
 - [13] S. Q. Murphy et al., Phys. Rev. Lett. **72**, 728 (1994).
 - [14] I. B. Spielman et al., Phys. Rev. Lett. **84**, 5808 (2000).
 - [15] I. B. Spielman et al., Phys. Rev. Lett. **87**, 036803 (2001).
 - [16] M. Kellogg et al., Phys. Rev. Lett. **88**, 126804 (2002).
 - [17] V. Pellegrini et al., Phys. Rev. Lett. **78**, 310 (1997).
 - [18] V. Pellegrini et al., Science **281**, 799 (1998).
 - [19] S. Das Sarma et al., Phys. Rev. Lett. **79**, 917 (1997).
 - [20] I. K. Marmorosk and S. Das Sarma, Phys. Rev. B **45**, 13396 (1992).
 - [21] A. S. Plaut et al., Phys. Rev. B **55**, 9282 (1997).
 - [22] Daw-Wei Wang et al., Phys. Rev. B **66**, 195334 (2002).
 - [23] M. M. Fogler and F. Wilczek, Phys. Rev. Lett. **86**, 1833 (2001).
 - [24] T. S. Lay et al., Phys. Rev. B **50**, 17725(R) (1994).
 - [25] M. Abolfath et al., Phys. Rev. B **61**, 4762 (2000).